RSC Advances

PAPER

View Article Online
View Journal | View Issue

Cite this: *RSC Adv.*, 2017, **7**, 10791

Amidoximated poly(vinyl imidazole)-functionalized molybdenum disulfide sheets for efficient sorption of a uranyl tricarbonate complex from aqueous solutions†

Liang Shen,[a] Xiaoli Han,[a] Jun Qian[a] and Daoben Hua*[ab]

Received 11th December 2016
Accepted 30th January 2017

DOI: 10.1039/c6ra28051j

rsc.li/rsc-advances

It is of strategic importance to capture uranium(VI) from aqueous solutions from the points of environment and energy. A new method is reported herein for efficient uranium(VI) capture from aqueous solutions by amidoximated poly(vinyl imidazole)-functionalized MoS_2 sheets. Specifically, the sorbent is prepared by grafting amidoximated poly(vinyl imidazole) onto MoS_2-sheets through covalent bonds. The sorption follows pseudo-second-order kinetics and the equilibrium can be reached within 30 s. There is a large sorption capacity of 348.4 mg g^{-1} at pH 8.0 and 298.15 K. The sorbent shows good selectivity towards uranium(VI) over the coexisting ions in comparison with bare MoS_2-sheets. In addition, the sorbent exhibits remarkable salt-resistant stability and can be regenerated efficiently after five cycles with high cycle efficiency. To the best of our knowledge, this is the first report on MoS_2 sheets for uranium(VI) sorption with high efficiency from aqueous solution.

Introduction

Nowadays there are 436 nuclear power units with a capacity of about 370 million kilowatts in the world. Uranium is one of the primary fuel sources in the generation of nuclear energy. As estimated by the International Atomic Energy Agency, the total identified uranium resources on land can only last for about a century.[1] The quantity of uranium in the oceans (*i.e.* ~4.5 billion tons) is 1000 times higher than that in terrestrial ores.[2,3] If uranium in seawater can be economically extracted, it will be enough for sustainable utilization of nuclear energy over the next few centuries. Therefore, it is a critical subject to efficiently capture uranium from aqueous solution including seawater.[4,5]

Over the past years, many researchers have studied the recovery of uranium from aqueous solutions, such as extraction,[3] ion exchange,[6] co-precipitation,[7] flotation,[8] membrane filtration,[9] and sorption.[3,10] Among them, sorption is widely utilized for uranium separation due to easy operation and low operating cost. Many sorbents of various matrix have been investigated, such as mesoporous carbon,[11,12] chelating polymers,[13,14] graphene oxides,[15–17] metal sulfides,[18,19] engineered proteins,[20] and metal–organic frameworks.[21] Although considerable achievements have been made, it is still a challenge to effectively extract uranium from aqueous solutions due to the complexity of environment, such as low concentration, a large number of coexisting ions, and high salinity.[2,22] Therefore, it is still important to develop new materials for uranium capture from aqueous solutions.

Layered MoS_2 is one kind of graphene-like two-dimensional materials with a structure of "S–Mo–S" sandwich. Ascribed to excellent mechanical properties and chemical stability,[23–26] MoS_2 has gained significant interest for several applications: electronic transistors,[24,27] lubrication,[26] catalysis,[25] energy storage,[28] sensors,[29] and sorption.[30,31] For instance, Chao *et al.*[30] prepared graphene-like layered MoS_2 by hydrothermal method for efficiently eliminating doxycycline antibiotic from aqueous solution; and Massey *et al.*[31] reported hierarchical microspheres of MoS_2 nanosheets for fast and efficient removal of dyes from the wastewater. Obviously, MoS_2-sheets may be promising matrix materials for efficient uranium sorption from aqueous solution. However, the application of MoS_2-sheets for metal sorption, especially for radionuclide treatment, has not been explored until now.

Uranyl tricarbonate complex $[UO_2(CO_3)_3]^{4-}$ is the most abundant species of uranium(VI) in aqueous solutions with high $[CO_3^{2-}]$ and pH.[32] Zeng *et al.*[33] recently grafted cationic poly(amidoxime) onto polypropylene nonwoven fabric for extraction of $[UO_2(CO_3)_3]^{4-}$ from aqueous solution. We noticed that

[a]*School for Radiological and Interdisciplinary Sciences (RAD-X), College of Chemistry, Chemical Engineering and Materials Science, Soochow University, Suzhou 215123, China. E-mail: dbhua_lab@suda.edu.cn; Fax: +86-512-65883261*

[b]*Collaborative Innovation Center of Radiological Medicine of Jiangsu Higher Education Institutions, Suzhou 215123, China*

† Electronic supplementary information (ESI) available: Synthesis of DDATC, PVIAO and MoS_2-sheets, sorption kinetics and isotherms, comparison of rate constant, elemental analysis, distribution of U(VI) species, SEM images, zeta potential, and particles size distributions of MoS_2 samples. See DOI: 10.1039/c6ra28051j

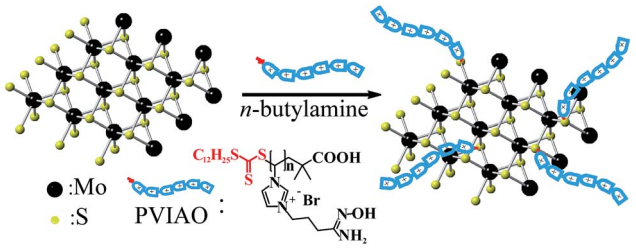

Scheme 1 The schematic for synthesis of PVIAO-modified MoS_2-sheets.

positively charged sorbents can attract the negative uranium(VI) complex while repelling the other cations, subsequently leading to a higher sorption selectivity and faster sorption rate.[33,34] Inspired by this finding, we herein synthesized amidoximated poly(vinyl imidazole)-functionalized MoS_2 sheets (MoS_2-PVIAO) for uranium(VI) capture from aqueous solutions (Scheme 1).

Specifically, the sorbent was prepared by one-pot reaction of amidoximated poly(vinyl imidazole) (PVIAO) and MoS_2-sheets in the presence of *n*-butylamine. During the reaction, the terminal trithiocarbonate groups of PVIAO were converted into thiol groups by aminolysis reaction,[35] and the polymers can graft onto exfoliated MoS_2-sheets through disulphide bonds[29,36] and Coulomb interaction.[37] The high surface area of MoS_2-sheets would bring about a faster sorption.[31] Furthermore, the positive charges of PVIAO can improve the sorption selectivity of uranyl tricarbonate complex.[33,34] Therefore, it is expected that the sorbent MoS_2-PVIAO could be used for effective uranium(VI) sorption from aqueous solutions.

Experimental

Materials and methods

1-Vinylimidazole (VI, CP), 2,2′-azoisobutyronitrile (AIBN, CP), sodium sulfite anhydrous (Na_2SO_3, AR) and *n*-butylamine (99%, AR) were bought from Sinopharm Chemical Reagent Co., Ltd. 4-Bromobutyronitrile (97%) and hydroxylamine hydrochloride ($NH_2OH \cdot HCl$, 99%) were obtained from J&K Chemical Co., Ltd. *n*-Butyllithium solution (1.6 mol L^{-1}) in hexane was purchased from Adamas Reagent Co., Ltd. MoS_2 (98.5%, GR) was purchased from Acros Organics Co., Ltd.

VI was pretreated by reduced pressure distillation and stored at −18 °C prior to use. AIBN was purified by recrystallization from 95% ethanol. ($UO_2(NO_3)_2 \cdot 6H_2O$), (Fluka, AR) was dissolved to prepare the stock solutions of uranyl ions. *S*-1-Dodecyl-*S*′-(α,α′-dimethyl-α″-acetic acid)trithiocarbonate (DDATC) was prepared in accordance to the previous literature[38] (Fig. S1, ESI†). All other reagents and chemicals were used as received. The characterization methods were shown in ESI.†

Synthesis of MoS_2-PVIAO

MoS_2-sheets were first exfoliated by intercalation with *n*-butyllithium[36] (ESI†), and PVIAO (M_n = 2900 g mol^{-1}, PDI = 1.08) was prepared by RAFT polymerization (Fig. S2, ESI†). A typical synthetic method for MoS_2-PVIAO was shown as follows: specifically, MoS_2-sheets (0.2 g, 1.25 mmol) were dispersed in 200 mL of ultrapure water. Then, Na_2SO_3 (1.0 g, 7.93 mmol) and PVIAO (0.2 g, 0.07 mmol) were added into suspension with continuously stirring under an argon atmosphere for 0.5 h at room temperature. 2.0 mL of *n*-butylamine was injected into the mixture and then sonicated for 2 h. After the mixture was agitated for extra 20 h, it was dialyzed against continuous water flow with dialysis membranes (MWCO = 10 K). Then it was lyophilized to give the final black powder. For comparison, MoS_2-PVIAO samples with different grafting degree (GD) were also prepared by the similar experiment and the recipes were shown in Table 1.

Table 1 Synthesis recipes of MoS_2-PVIAO and graft degree of PVIAO

Sample	MoS_2-sheets (g)	Na_2SO_3 (g)	*n*-Butylamine (mL)	PVIAO (g)	GD[a]
MoS_2-PVIAO-1	0.20	1.0	2.0	0.10	10.0%
MoS_2-PVIAO-2	0.20	1.0	2.0	0.20	17.1%
MoS_2-PVIAO-3	0.20	1.0	2.0	0.50	53.7%

[a] Graft degree was determined by TGA curve.

Sorption experiments

The distribution of uranium(VI) species was calculated using Medusa program under different pH conditions (Fig. S3A, ESI†), and the result showed uranyl tricarbonate complex is the dominant species of uranium(VI) in aqueous solutions when pH ≥ 8.0. Therefore, all sorption experiments were conducted at pH 8.0 and 298.15 K in polyethylene tubes. The pH values were adjusted by 2.0 mol L^{-1} HNO_3 and 2.0 mol L^{-1} Na_2CO_3 solutions. The uranyl concentrations before and after sorption were analyzed by ICP-MS. The equilibrium sorption amount (q_e) and sorption efficiency (SE) were determined based on eqn (1) and (2), respectively:

$$q_e = (C_0 - C_e)\frac{V}{M} \quad (1)$$

$$\mathrm{SE}\ (\%) = \frac{C_0 - C_e}{C_0} \times 100 \quad (2)$$

where C_0 and C_e (mg L^{-1}) represent the initial and final uranium concentrations, respectively. M (g) represents the desiccative sorbent weight, and V (L) denotes the volume of aqueous solution.

The first set of experiments was performed to demonstrate the effect of sorbent dose (0.03–2.00 g L^{-1}) on uranium(VI) sorption with an initial concentration of 5.0×10^{-5} mol L^{-1}. After shaking for 24 h until sorption equilibrium, the solid phase was separated by centrifugation.

The second set of experiments was conducted to check into the effect of contact time on the sorption of uranium(VI). Since the sorption equilibrium was achieved in a short time, the mixture was filtered immediately after sorption within different time.

The third set of experiments was carried out to examine the influence of various coexisting ions, salinity and different uranyl

initial concentrations (5.0×10^{-5} to 3.3×10^{-4} mol L^{-1}). A typical sorption procedure was described as follows: the sorbents (1.0 mg) were added into 5.0 mL of uranium(VI) solution and the mixture was shaking for 8 h until sorption equilibrium, and the sorbents were then removed by centrifugation. In addition, the total concentration of CO_3^{2-} was close to 6.0×10^{-3} mol L^{-1} when pH was adjusted to ~8.0 with Na_2CO_3 solutions. According to calculation with Medusa program, there is no precipitation of uranium(VI) in the solution under the experimental conditions (*i.e.* pH 8.0, $[CO_3^{2-}] = 6.0 \times 10^{-3}$ mol L^{-1}, and $[U] = 3.3 \times 10^{-4}$ mol L^{-1}) (Fig. S3B, ESI†).

Desorption and regeneration experiment

The desorption and regeneration studies were conducted to assess the recyclability of the sorbent. The as-prepared MoS_2-PVIAO (17.1%) powders (3.0 mg) were added into 10.0 mL of uranium(VI) solution under continuous oscillation. After saturated sorption, the mixture was dialyzed in HCl solution (0.1 mol L^{-1}, 200 mL) and $NaHCO_3$ solution (1.0 mol L^{-1}, 200 mL) to remove uranium(VI), respectively. Ultrapure water (200 mL) was then used to wash for three times until neutral and lyophilized for reuse.

Simulated seawater experiment

Simulated seawater experiments were conducted with two models according to the ref. 12. Specifically, the simulated seawater was comprised of 0.438 mol L^{-1} NaCl, 2.297 mmol L^{-1} $NaHCO_3$ and 0.034 mmol L^{-1} uranyl nitrate in ultrapure water. In addition, $CaCl_2$ (0.01 mmol L^{-1}) was also added into the solution to investigate the effect of calcium ions on sorption. The pH was adjusted to 8.0. MoS_2-PVIAO (17.1%) (1.0 mg) and 5.0 mL of stock solution were placed in polyethylene tubes. The mixture was shaken for different period of time at room temperature. Finally the sorbents were removed by filtration.

Results and discussion

Characterization of MoS_2-PVIAO

In order to synthesize MoS_2-PVIAO, MoS_2-sheets were first prepared by intercalating exfoliation of MoS_2 powder with *n*-butyllithium,[36] and PVIAO was synthesized by controlled polymerization of VI and subsequent reaction with 4-bromobutyronitrile and with hydroxylamine, respectively (ESI†). MoS_2-PVIAO was then prepared by grafting PVIAO onto MoS_2-sheets in the presence of *n*-butylamine. During the reaction, the terminal trithiocarbonate groups of PVIAO chains were converted into thiol groups, and the chains could connect with vacancy defects of exfoliated MoS_2-sheets through disulphide bonds and Coulomb interaction.

The morphological features of MoS_2-PVIAO were characterized by TEM and XRD. In comparison with MoS_2 (Fig. 1A), the sheets of MoS_2-PVIAO present obvious nano-sheets structure and the interlayer distance was about 1.0 nm (Fig. 1B and the inset). Furthermore, the better dispersion of MoS_2-PVIAO indicated the successful graft of PVIAO onto MoS_2-sheets (Fig. 1C). This point was further demonstrated by XRD patterns. After

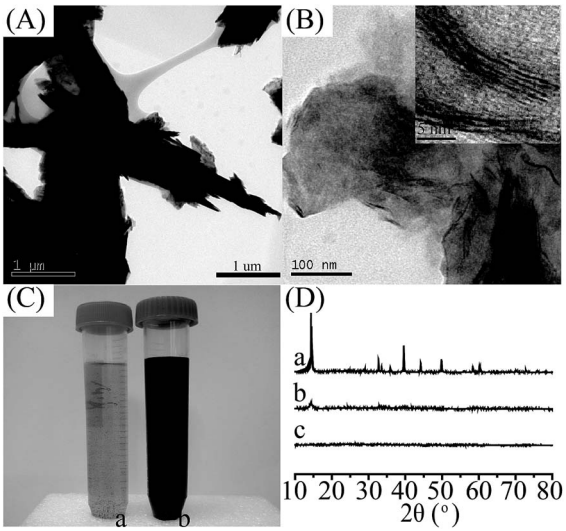

Fig. 1 (A) TEM images of MoS_2 (scale bar: 1 μm); (B) TEM images of MoS_2-PVIAO (scale bar: 100 nm). Inset: an edge of individual MoS_2-PVIAO (scale bar: 5 nm); (C) pictures of (a) MoS_2-sheets and (b) MoS_2-PVIAO (17.1%) (2.0 mg of solid was dispersed in 10.0 mL of water). (D) XRD powder patterns for (a) MoS_2, (b) MoS_2-sheets, and (c) MoS_2-PVIAO (17.1%).

exfoliation and modification of MoS_2, the characteristic peaks at $2\theta = 13°$ and 41° for MoS_2 (JCPDS card 37-1492) disappeared (Fig. 1D), suggesting the crystal structure was destroyed by polymer chains.

The chemical components of MoS_2-PVIAO (17.1%) were characterized by XPS and FT-IR spectra. XPS scans showed the elements in MoS_2-sheets and MoS_2-PVIAO (17.1%), respectively (Fig. 2A). Compared with MoS_2-sheets (Fig. 2A, trace a), MoS_2-PVIAO (17.1%) (Fig. 2A, trace b) showed the new peak for N (1s) element, which could be curve-fitted with three peak components ascribed to C–N, C=N, and N–O species (Fig. 2B), suggesting the successful grafting of PVIAO onto MoS_2-sheets. The chemical structures of MoS_2-PVIAO (17.1%) were confirmed by FT-IR spectra (Fig. 2C, trace b). Compared with MoS_2-sheets (Fig. 2C, trace a), the characteristic bands of C=N (ring, 1539 cm^{-1}), N–O (835 cm^{-1}) occurred for MoS_2-PVIAO (Fig. 2C, trace b). Moreover, MoS_2-PVIAO were positively charged after the graft of cationic polymer (Fig. S4, ESI†), and the more graft content, the higher zeta potential, which would be helpful for the sorption of negative uranyl complex.

In order to investigate chemical contents of MoS_2-PVIAO, thermogravimetric analysis was carried out. The result was shown in Fig. 2D. There were two obvious stages during the process of mass loss: crystal water desorbed at stage I, whose weight percentage was approximately 2.2%; stage II was the process of decomposition of PVIAO, which can be used to determine the graft contents as 10.0%, 17.1% and 53.7% for MoS_2-PVIAO, respectively.

Effects of sorbent dose on sorption

The influence of sorbent amount on uranium(VI) sorption was conducted at pH 8.0 and 298.15 K. The result was shown in

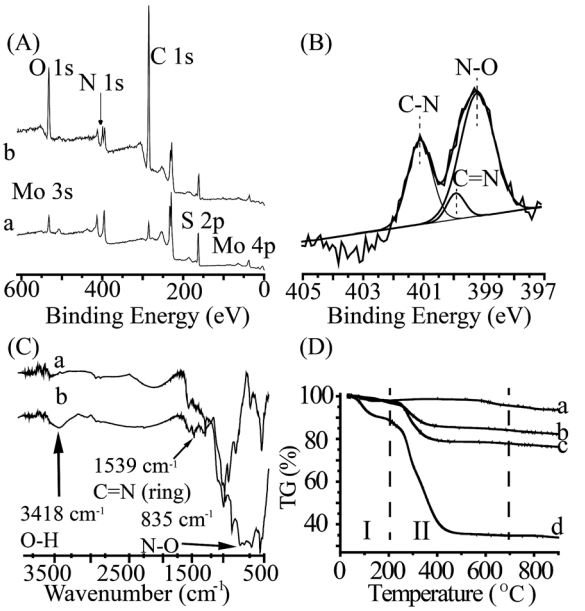

Fig. 2 (A) XPS spectra of (a) MoS_2-sheets and (b) MoS_2-PVIAO (17.1%); (B) XPS spectra of N 1s of MoS_2-PVIAO (17.1%); (C) FT-IR spectra of (a) MoS_2-sheets and (b) MoS_2-PVIAO (17.1%). (D) TGA curves of (a) MoS_2-sheets, (b) MoS_2-PVIAO (10.0%), (c) MoS_2-PVIAO (17.1%) and (d) MoS_2-PVIAO (53.7%).

Fig. 3A. With the increase of sorbent dose, sorption efficiency was first increased and then decreased, and there is a maximum value at 0.20 g L^{-1}. The result may be attributed that the stacking of MoS_2-sheets at high concentration, resulting in a reduction of the sorption efficiency. To confirm the speculation, SEM and particle size distributions were conducted for MoS_2-PVIAO (17.1%) with different sorbent doses (Fig. S5, ESI†). The aggregation of the sorbents can be recorded obviously and particle size distributions were increasing with the sorbent dose. Therefore, the optimum sorbent dose of 0.20 g L^{-1} was selected for next experiments.

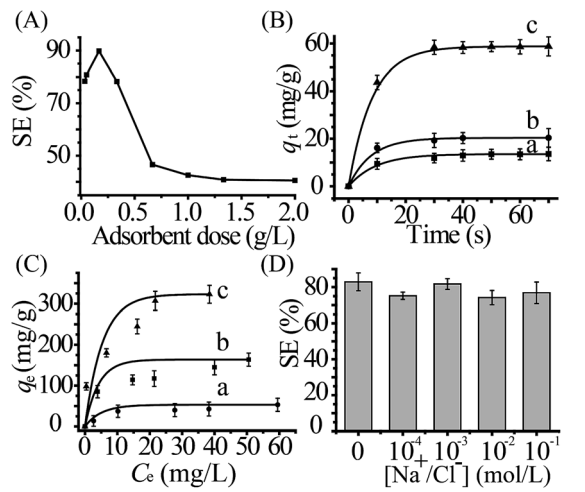

Fig. 3 (A) The relationship between sorption efficiency and sorbent dose (0–60 mg L^{-1}) in uranium(VI) sorption by MoS_2-PVIAO (17.1%). (B) Effects of contact time on uranium(VI) sorption with 0.2 g L^{-1} sorbent dose: (a) MoS_2-sheets, (b) MoS_2-PVIAO (10.0%) and (c) MoS_2-PVIAO (17.1%). (C) Sorption isotherm plots for uranium(VI) sorption with 0.2 g L^{-1} sorbent dose: (a) MoS_2-sheets, (b) MoS_2-PVIAO (17.1%) and (c) MoS_2-PVIAO (53.7%). (D) The sorption efficiency of uranium(VI) by MoS_2-PVIAO (17.1%, 0.2 g L^{-1} sorbent dose) in the presence of Na^+/Cl^- with different concentrations (experimental condition: 5.0 mL solution, pH 8.0, 5.0×10^{-5} mol L^{-1} uranium(VI) and 298.15 K).

Sorption kinetics

To investigate the sorption rate, the kinetic experiments were performed at pH 8.0 and 298.15 K with the optimum sorbent dose of 0.20 g L^{-1}. The result was shown in Fig. 3B. The effect of contact time (t) on uranium(VI) sorption showed that all of the sorption reached equilibrium within 30 s, and the more grafting polymer, the more equilibrium amount.

Pseudo-first-order equation[39] and pseudo-second-order equation[40,41] were used to simulate the sorption kinetics (Fig. S6, ESI†), and the kinetics parameters were listed in Table 2. Kinetic profiles were appropriately described by pseudo-second-order model due to the larger correlation coefficients (R^2) and the more accurate calculated q_e. Importantly, there was a remarkably larger rate constant k_2 of MoS_2-PVIAO compared with the reference results (Table S1, ESI†). It was also noticed that the k_2 for MoS_2-PVIAO (10.0%) was slightly larger than MoS_2-sheets, implying a more rapid sorption, which may be ascribed to electrostatic attraction between the positive sorbent and negative uranyl tricarbonate complex besides the good covalency between uranium and sulfur.[18,19] However, the k_2 for MoS_2-PVIAO (17.1%) was much smaller than MoS_2-PVIAO (10.0%), which may be attributed to the weaken interaction of MoS_2 with uranium(VI) by relatively more polymer chains.

Sorption isotherm

To understand sorption capacity, the isotherm studies were carried out with the concentrations of uranium(VI) from 5.0×10^{-5} to 3.3×10^{-4} mol L^{-1} at 298.15 K and pH 8.0. The relationship between q_e and C_e was shown in Fig. 3C. The sorption data were simulated with Langmuir and Freundlich models[42,43] (Fig. S7, ESI†).

The correlation coefficients and parameters were summarized in Table 3. The sorption process was more appropriately described by Langmuir model according to the larger correlation coefficients (R^2). The result may be ascribed to that active sites homogenously distribute on the surfaces, thereby leading to monolayer sorption. The capacity q_{max} of MoS_2-PVIAO (53.7%) could reach 348.4 mg g^{-1}, which was far larger than that of MoS_2-sheets (57.97 mg g^{-1}). In addition, there was a larger b value for MoS_2-PVIAO than that for MoS_2-sheets, which may be ascribed to the Coulomb force between cationic sorbents and negative uranyl complex.

Effect of coexisting ions and salinity on uranium(VI) sorption

Considering that certain metals (Fe^{3+}, Zn^{2+}, *etc.*) may form precipitation at high [CO_3^{2-}] and pH,[44] the coexisting ions (Mg^{2+}, Ca^{2+}, K^+, SO_4^{2-}, Br^-, BO_3^{3-}, and VO_3^-) were selected for the experiments of uranium(VI) sorption to study the selectivity of MoS_2-PVIAO (17.1%). All the coexisting ions are in the same

Table 2 Kinetic parameters for the sorption of uranium(VI) by MoS_2-sheets, MoS_2-PVIAO (10.0%) and MoS_2-PVIAO (17.1%) (experimental condition: 5.0 mL solution, pH 8.0, 0.2 g L^{-1} sorbent dose, 5.0×10^{-5} mol L^{-1} uranium(VI) and 298.15 K)

	Pseudo-first order				Pseudo-second order		
Sample	$q_{e,exp}$ (mg g^{-1})	k_1 (s^{-1})	$q_{e,cal}$ (mg g^{-1})	R^2	k_2 (g mg^{-1} s^{-1})	$q_{e,cal}$ (mg g^{-1})	R^2
MoS_2-sheets	13.57	0.087	13.49	0.905	0.011	14.84	0.998
MoS_2-PVIAO (10.0%)	20.42	0.167	32.81	0.878	0.015	21.44	0.999
MoS_2-PVIAO (17.1%)	58.75	0.105	34.13	0.875	0.005	61.80	0.998

Table 3 Langmuir and Freundlich parameters for uranium(VI) sorption by MoS_2-sheets, MoS_2-PVIAO (17.1%) and MoS_2-PVIAO (53.7%) (experimental condition: 5.0 mL solution, pH 8.0, 0.2 g L^{-1} sorbent dose and 298.15 K)

	Langmuir			Freundlich		
Sorbent	q_{max} (mg g^{-1})	b (L mg^{-1})	R^2	K_F (mol^{1-n} L^n g^{-1})	N	R^2
MoS_2-sheets	57.97	0.109	0.963	10.72	2.482	0.843
MoS_2-PVIAO (17.1%)	178.6	0.133	0.967	59.78	4.127	0.954
MoS_2-PVIAO (53.7%)	348.4	0.249	0.964	121.5	3.758	0.962

concentration as those in the seawater.[33,45] The distribution ratio (K_d) can be calculated by eqn (3):

$$K_d = \frac{C_0 - C_e}{C_e} \times \frac{V}{m} \quad (3)$$

where C_0 and C_e (mg L^{-1}) are the concentrations of uranium(VI) in solution before and after sorption, respectively. V (L) represents the solution volume and m (g) is the mass of the sorbent.

The uranium(VI) uptake and the distribution ratio were listed in Table 4. The K_d of MoS_2-PVIAO (17.1%) for uranium(VI) was remarkably larger than that of bare MoS_2-sheets, indicating the higher sorption selectivity for MoS_2-PVIAO (17.1%). This result may be attributed to positive charges of PVIAO that can repel the other cations, which improves the selectivity for uranium(VI). It was also noticed that the uranium(VI) uptake decreased to some extent when Mg^{2+}, Ca^{2+} and VO_3^- existed, which may be attributed to the chemisorption of sulfur with the ions.

To study the effect of salinity on uranium(VI) sorption, different concentrations of NaCl (10^{-4} to 10^{-1} mol L^{-1}) were added for uranium(VI) sorption experiments. The result was depicted in Fig. 3D. The material remained a high sorption efficiency (76.8%) even at high salinity (0.1 mol L^{-1} NaCl), implying that the sorbent had a good salt resistance.

Regeneration studies

Regenerability is important for an effective and economical sorbent. In this study, the reusability of the sorbent was evaluated by five cycles of sorption/desorption using 0.1 mol L^{-1} HCl and 1.0 mol L^{-1} $NaHCO_3$ solution as eluents, respectively. The results were shown in Fig. 4A. There was only a slight decrease of cycle efficiency (CE) after five cycles using HCl or $NaHCO_3$ as eluents. In addition, elemental analysis was conducted for the sorbent after five cycles with 0.1 mol L^{-1} HCl eluent, and the result showed the nitrogen content slightly varied from 6.47% to 5.27% (Table S2, ESI†). The result might be attributed to a small amount of polymer on MoS_2-sheets by Coulomb interaction, which could be washed off by HCl solution. To evaluate structure transformation of the sorbents, the sorbents after five cycles were characterized by FT-IR (Fig. S8, ESI†), and no obvious change was observed in material structure after elution with HCl and $NaHCO_3$.

Table 4 Sorption of uranium(VI) on MoS_2-sheets and MoS_2-PVIAO (17.1%) in the presence of coexisting ions (experimental condition: 5.0 mL solution, pH 8.0, 0.2 g L^{-1} sorbent dose, a certain concentration of other ions, 5.0×10^{-5} mol L^{-1} uranium(VI) and 298.15 K)

			Uranium(VI) uptake (mg g^{-1})		Distribution ratio K_d (L g^{-1})	
No.	Salt added	Concentration mol L^{-1}	MoS_2-sheets	MoS_2-PVIAO (17.1%)	MoS_2-sheets	MoS_2-PVIAO (17.1%)
1	Not added	—	15.52	51.66	2.431	142.0
2	$MgCl_2$	5.2×10^{-2}	6.701	39.92	0.856	17.46
3	Na_2SO_4	2.7×10^{-2}	10.31	51.00	1.429	117.3
4	$CaCl_2$	9.9×10^{-3}	9.344	40.57	1.238	17.32
5	KCl	9.7×10^{-3}	13.10	48.38	1.974	63.66
6	KBr	8.0×10^{-4}	11.99	51.18	1.729	128.6
7	H_3BO_3	4.0×10^{-4}	11.41	44.87	1.592	133.4
8	NH_4VO_3	5.1×10^{-5}	14.84	30.22	0.924	43.51

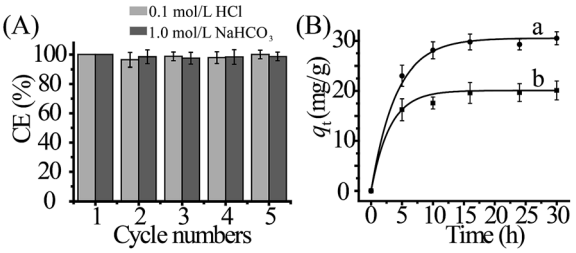

Fig. 4 (A) Recycling of MoS_2-PVIAO (17.1%) in the uranium(VI) sorption with different eluents: 0.1 mol L^{-1} HCl and 1.0 mol L^{-1} $NaHCO_3$ (experimental condition: 10.0 mL solution, pH 8.0, 3.0 mg sorbent, 5.0×10^{-5} mol L^{-1} uranium(VI) and 298.15 K). (B) The sorption amount of uranium(VI) with different period of contact time in simulated seawater: (a) without calcium ions, and (b) with 0.01 mmol L^{-1} calcium ions (experimental condition: 5.0 mL solution, pH 8.0, 0.2 g L^{-1} sorbent dose, 0.034 mmol L^{-1} uranium(VI), 0.438 mol L^{-1} of NaCl, 2.297 mmol L^{-1} of $NaHCO_3$ and 298.15 K).

Test with simulated seawater

Considering $[UO_2(CO_3)_3]^{4-}$ is the dominant form of uranium(VI) in seawater, simulated seawater experiments were conducted in this study. The influence of contact time (t) on sorption amount (q_t) was shown in Fig. 4B. It can be found that even at a lower uranium concentration with high salinity, the sorbent also can capture uranium(VI) within 10 h with a capacity of 28.6 mg g^{-1} at pH 8.0 and 298.15 K (Fig. 4Ba). When Ca^{2+} ions were present at the concentration of 0.01 mmol L^{-1}, q_{max} was slightly reduced from 28.6 mg g^{-1} to 20.1 mg g^{-1} (Fig. 4Bb), which may be due to the formation of the specie $Ca_2(UO_2)(CO_3)_3$.[46,47] The results indicated the sorbent may be used as a promising candidate for potential uranium(VI) extraction from seawater.

Conclusions

In summary, we show the amidoximated poly(vinyl imidazole)-functionalized MoS_2 sheets for efficient capture of uranyl tricarbonate complex from aqueous solutions. The sorbent was prepared by grafting amidoximated poly(vinyl imidazole) onto MoS_2-sheets. The effects of sorbent dose, sorption kinetics and isotherms, coexisting ions and salinity on uranium(VI) sorption were studied. The sorption follows pseudo-second-order kinetics model with larger rate constant, and the equilibrium can be reached within 30 s. The maximum sorption capacity can reach 348.4 mg g^{-1} at pH 8.0 and 298.15 K. The MoS_2-PVIAO (17.1%) showed higher selectivity towards uranium(VI) over coexisting ions in comparison with MoS_2-sheets. In addition, the sorbent exhibited remarkable salt-resistant stability and could be regenerated efficiently after five cycles with high sorption efficiency. As far as we know, this is the first report on MoS_2-sheets for sorption of radionuclides from aqueous solution. This work demonstrates that MoS_2-sheets can be used as the promising matrix materials for the separation of radionuclide from aqueous solution.

Acknowledgements

This work is supported by Natural Science Foundation of China (U1532111, 91326202), a Project Funded by the Priority Academic Program Development of Jiangsu Higher Education Institutions (PAPD), and Jiangsu Key Laboratory of Radiation Medicine and Protection.

References

1 Uranium 2011, *Resourses, Production and Demand, NEA No. 7059*, Organisation for Economic Co-operation and Development/Nuclear Energy Agency, International Atomic Energy Agency, 2012.
2 Y. Lu, *Nat. Chem.*, 2014, **6**, 175–177.
3 R. V. Davies, J. Kennedy, R. W. Mcilroy, R. Spence and K. M. Hill, *Nature*, 1964, **203**, 1110–1115.
4 D. Beltrami, G. Cote, H. Mokhtari, B. Courtaud, B. A. Moyer and A. Chagnes, *Chem. Rev.*, 2014, **114**, 12002–12023.
5 F. P. Carvalho, J. M. Oliveira, I. Lopes and A. Batista, *J. Environ. Radioact.*, 2007, **98**, 298–314.
6 M. J. Manos and M. G. Kanatzidis, *J. Am. Chem. Soc.*, 2012, **134**, 16441–16446.
7 A. Baeza, M. Fernandez, M. Herranz, F. Legarda, C. Miro and A. Salas, *Water, Air, Soil Pollut.*, 2006, **173**, 57–69.
8 T. P. Rao, P. Metilda and J. M. Gladis, *Talanta*, 2006, **68**, 1047–1064.
9 A. Dâas and O. Hamdaoui, *J. Membr. Sci.*, 2010, **355**, 214.
10 I. Tabushi, Y. Kobuke and T. Nishiya, *Nature*, 1979, **280**, 665–666.
11 Y. F. Yue, X. G. Sun, R. T. Mayes, J. Kim, P. F. Fulvio, Z. A. Qiao, S. Brown, C. Tsouris, Y. Oyola and S. Dai, *Sci. China: Chem.*, 2013, **56**, 1510–1515.
12 J. Gorka, R. T. Mayes, L. Baggetto, G. M. Veith and S. Dai, *J. Mater. Chem. A*, 2013, **1**, 3016–3026.
13 S. Das, S. Brown, R. T. Mayes, C. J. Janke, C. Tsouris, L. J. Kuo, G. Gill and S. Dai, *Chem. Eng. J.*, 2016, **298**, 125–135.
14 T. S. Anirudhan, A. R. Tharun, S. Rijith and P. S. Suchithra, *J. Appl. Polym. Sci.*, 2011, **122**, 874–884.
15 Y. B. Sun, C. C. Ding, W. C. Cheng and X. K. Wang, *J. Hazard. Mater.*, 2014, **280**, 399–408.
16 Y. B. Sun, D. D. Shao, C. L. Chen, S. B. Yang and X. K. Wang, *Environ. Sci. Technol.*, 2013, **47**, 9904–9910.
17 L. Shao, X. F. Wang, Y. M. Ren, S. F. Wang, J. R. Zhong, M. F. Chu, H. Tang, L. Z. Luo and D. H. Xie, *Chem. Eng. J.*, 2016, **286**, 311–319.
18 S. L. Ma, L. Huang, L. J. Ma, Y. Shim, S. M. Islam, P. L. Wang, L. D. Zhao, S. C. Wang, G. B. Sun, X. J. Yang and M. G. Kanatzidis, *J. Am. Chem. Soc.*, 2015, **137**, 3670–3677.
19 L. J. Ma, Q. Wang, S. M. Islam, Y. C. Liu, S. L. Ma and M. G. Kanatzidis, *J. Am. Chem. Soc.*, 2016, **138**, 2858–2866.
20 L. Zhou, M. Bosscher, C. S. Zhang, S. Ozcubukcu, L. Zhang, W. Zhang, C. J. Li, J. Z. Liu, M. P. Jensen, L. H. Lai and C. He, *Nat. Chem.*, 2014, **6**, 236–241.
21 M. Carboni, C. W. Abney, S. Liu and W. Lin, *Chem. Sci.*, 2013, **4**, 2396–2402.
22 J. Kim, C. Tsouris, R. T. Mayes, Y. Oyola, T. Saito, C. J. Janke, S. Dai, E. Schneider and D. Sachde, *Sep. Sci. Technol.*, 2013, **48**, 367–387.
23 Y. P. V. Subbaiah, K. J. Saji and A. Tiwari, *Adv. Funct. Mater.*, 2016, **26**, 2046–2069.

24 J. Q. Liu, Z. Y. Zeng, X. H. Cao, G. Lu, L. H. Wang, Q. L. Fan, W. Huang and H. Zhang, *Small*, 2012, **8**, 3517–3522.
25 L. Liao, J. Zhu, X. J. Bian, L. N. Zhu, M. D. Scanlon, H. H. Girault and B. H. Liu, *Adv. Funct. Mater.*, 2013, **23**, 5326–5333.
26 L. Rapoport, N. Fleischer and R. Tenne, *J. Mater. Chem.*, 2005, **15**, 1782–1788.
27 T. Y. Wang, L. Liu, Z. W. Zhu, P. Papakonstantinou, J. B. Hu, H. Y. Liu and M. X. Li, *Energy Environ. Sci.*, 2013, **6**, 625–633.
28 J. N. Coleman, M. Lotya, A. O'Neill, S. D. Bergin, P. J. King, U. Khan, K. Young, A. Gaucher, S. De, R. J. Smith, I. V. Shvets, S. K. Arora, G. Stanton, H. Y. Kim, K. Lee, G. T. Kim, G. S. Duesberg, T. Hallam, J. J. Boland, J. J. Wang, J. F. Donegan, J. C. Grunlan, G. Moriarty, A. Shmeliov, R. J. Nicholls, J. M. Perkins, E. M. Grieveson, K. Theuwissen, D. W. McComb, P. D. Nellist and V. Nicolosi, *Science*, 2011, **331**, 568–571.
29 H. Cheng, N. Dong, T. Bai, Y. Song, J. Wang, Y. Qin, B. Zhang and Y. Chen, *Chemistry*, 2016, **22**, 4500–4507.
30 Y. H. Chao, W. S. Zhu, X. Y. Wu, F. F. Hou, S. H. Xun, P. W. Wu, H. Y. Ji, H. Xu and H. M. Li, *Chem. Eng. J.*, 2014, **243**, 60–67.
31 A. T. Massey, R. Gusain, S. Kumari and O. P. Khatri, *Ind. Eng. Chem. Res.*, 2016, **55**, 7124–7131.
32 T. Hiemstra, W. H. V. Riemsdijk, A. Rossberg and K. U. Ulrich, *Geochim. Cosmochim. Acta*, 2009, **73**, 4437–4451.
33 Z. H. Zeng, Y. Q. Wei, L. Shen and D. B. Hua, *Ind. Eng. Chem. Res.*, 2015, **54**, 8699–8705.
34 Y. Wei, J. Qian, L. Huang and D. Hua, *RSC Adv.*, 2015, **5**, 64286–64292.
35 D. B. Hua, L. J. Kuang and H. J. Liang, *J. Am. Chem. Soc.*, 2011, **133**, 2354–2357.
36 S. S. Chou, M. De, J. Kim, S. Byun, C. Dykstra, J. Yu, J. X. Huang and V. P. Dravid, *J. Am. Chem. Soc.*, 2013, **135**, 4584–4587.
37 A. S. Goloveshkin, I. S. Bushmarinov, A. A. Korlyukov, M. I. Buzin, V. I. Zaikovskii, N. D. Lenenko and A. S. Golub, *Langmuir*, 2015, **31**, 8953–8960.
38 J. T. Lai, A. Debby Filla and R. Shea, *Macromolecules*, 2002, **35**, 6754–6756.
39 K. Saito, K. Uezu, T. Hori, S. Furusaki, T. Sugo and J. Okamoto, *AIChE J.*, 1988, **34**, 411–416.
40 Y. S. Ho, *J. Hazard. Mater.*, 2006, **136**, 681–689.
41 Y. S. Ho and G. McKay, *Chem. Eng. J.*, 1998, **70**, 115–124.
42 M. J. Temkin and V. Pyzhev, *Acta Physicochim. URSS*, 1940, **12**, 217–222.
43 H. Freundlich, *Z. Phys. Chem.*, 1906, **57**, 385–470.
44 A. J. Rubin and J. D. Johnson, *Anal. Chem.*, 1967, **39**, 298–302.
45 M. Biesalski and J. Ruhe, *Macromolecules*, 2002, **35**, 499–507.
46 A. O. Tirler and T. S. Hofer, *Dalton Trans.*, 2016, **45**, 4983–4988.
47 W. H. Wu, C. Priest, J. W. Zhou, C. J. Peng, H. L. Liu and D. E. Jiang, *J. Phys. Chem. B*, 2016, **120**, 7227–7233.